Organic Process Research & Development **2004**, *8*, 213−218

Resolution of 1,2-Diols by Enzyme-Catalyzed Oxidation with Anodic, Mediated Cofactor Regeneration in the Extractive Membrane Reactor: Gaining Insight by Adaptive Simulation

Daniela Degenring,[†,‡] Iris Schröder,[†,§] Christian Wandrey,[†] Andreas Liese,*[,†,∥] and Lasse Greiner[†,⊥]

Institut für Biotechnologie, Forschungszentrum Jülich, 52425 Jülich, Germany

Abstract:

Oxidative racemic resolution of 1,2-diols is a method for the synthesis of enantiopure diols not easily accessed by reduction. The constraints generally found for oxidation to hydroxy ketones can be overcome by coupling various techniques. To circumvent product inhibition, a membrane reactor with solvent extraction of the lipophilic product was chosen. For the oxidative regeneration of NAD^+ from NADH anodic oxidation mediated by ABTS was used. The kinetic characteristics of the system were determined independently for each significant system step. However, it proved difficult to simulate the coupled process completely with the kinetic data obtained independently, as true reaction conditions are not covered by kinetic experiments. A mixed approach using a system of ordinary differential equations corrected with data from the process (e.g. enzyme activity) leads to a satisfactory description. This model was applied as a starting point for identifying the relevant process parameters.

1. Introduction

Oxidoreductases are versatile biocatalysts; dehydrogenases in particular catalyze oxidations and reductions of interest to organic chemists and the fine chemical industry.[1−3] However, the effective application of dehydrogenases is often limited for reasons affecting this class of catalysts in general.[4,5]

Since the majority of dehydrogenases use a cofactor as redox equivalents, their in situ regeneration has to be considered for cost reasons. Additionally, kinetic inhibition by either the oxidized or reduced form must be overcome. Amongst the numerous methods for oxidative regeneration, electrochemical regeneration by mediated anodic oxidation is one of the most successful.[6,7]

A further kinetic complication for these biotransformations is the inhibition of the enzymes by carbonyl compounds. The concentration of the inhibitor must be low for the reaction to commence at reasonable rate. One possibility of overcoming product inhibition is the use of an extractive enzyme membrane reactor (EEMR).[8−16] The hydrophobic product is extracted with an organic solvent conveniently using a phase contactor module, whilst the enzyme is retained by means of ultrafiltration.[11,12]

Suitable and versatile catalysts still have to be discovered for the preparation of *S*-enantiomers of 1,2-diols via reduction of ketones. Until then kinetic racemic resolution by oxidation is the method of choice,[13] since these enzymes are commercially available at reasonable cost.[1]

The approaches of electrochemical regeneration of NAD^+ [14−18] and extraction[19,20] were combined in the electrochemical extractive enzyme membrane reactor (E^3MR) for the oxidative racemic resolution of a 1,2-diol with glycerol dehydrogenase from *Cellulomonas* spp. (GDH, EC 1.1.1.6).[19,2121] For the cofactor regeneration indirect electrochemical oxidation of NADH to NAD^+ mediated by the $ABTS^{2-}/ABTS^{\bullet-}$ redox couple (2,2′-azinobis(3-ethylbenzothiazoline-6-sulfonate) was used.[22] It was found to be a

* Corresponding author. E-mail: aliese@uni-muenster.de. http://www.uni-muenster.de/Chemie/BC/.

† Institut für Biotechnologie, Forschungszentrum Jülich.

‡ Present address: Institut für Informatik, Universität Rostock, Albert-Einstein Strasse 21, 18059 Rostock, Germany.

§ Present address: Lehrstuhl für Prozesstechnik, Universität des Saarlands, Im Stadtwald Geb. 47, 66123 Saarbrücken, Germany.

∥ Present address: Institut für Biochemie, Universität Münster, Wilhelm-Klemm-Str. 2, 48149 Münster, Germany.

⊥ Present address: Institut für Technische und Makromolekulare Chemie, RWTH Aachen, Worringerweg 1, 52074 Aachen, Germany.

(1) Hummel, W. *Trends in Biotechnology* **1999**, *17*, 487−492.
(2) Devaux-Basseguy, R.; Bergel, A.; Comtat, M. *Enzymol. Microbiol. Technol.* **1997**, *20*, 248−258.
(3) Wong, C.-H.; Whitesides, G. M. *Enzymes in synthetic organic chemistry*; Elsevier Science Ltd.: Oxford, 1994; p 370.
(4) Lee, L. G.; Whitesides, G. M. *J. Org. Chem.* **1986**, *51*, 25−36.
(5) Liese, A.; Zelinski, T.; Kula, M.-R.; Wandrey, C. *J. Mol. Catal. B: Enzym.* **1998**, *4*, 91−99.
(6) Steckhan, E.; Arns, T.; Heineman, W. R.; Hilt, G.; Hoormann, D.; Jörissen, J.; Kröner, L.; Lewall, B.; Pütter, H. *Chemosphere* **2001**, *43*, 63−73.
(7) Hollmann, F.; Witholt, B.; Schmid, A. *J. Mol. Catal. B: Enzym.* **2002**, *19−20*, 167−176.
(8) Kruse, W.; Hummel, W.; Kragl, U. *Recl. Trav. Chim. Pays-Bas* **1996**, *115*, 239−243.
(9) Wichmann, R.; Wandrey, C.; Bückmann, A. F.; Kula, M.-R. *Biotechnol. Bioeng.* **1981**, *23*, 2789−2802.
(10) Brielbeck, B.; Frede, M.; Steckhan, E. *Biocatalysis* **1994**, *10*, 49−64.
(11) Shin, J.-S.; Kim, B.-G.; Liese, A.; Wandrey, C. *Biotechnol. Bioeng.* **2001**, *73*, 179−187.
(12) Kragl, U.; Vasic-Racki, D.; Wandrey, C. *Chem.-Ing.-Technol.* **1992**, *64*, 499−509.
(13) Keith, J. M.; Larrow, J. F.; Jacobson, E. N. *Adv. Synth. Catal.* **2002**, *343*, 5−26.
(14) Allen, P. M.; Bowen, W. R. *Trends Biotechnol.* **1985**, *3*, 145−149.
(15) Laval, J.-M.; Bourdillon, C. *Biotechnol. Bioeng.* **1987**, *30*, 157−159.
(16) Steckhan, E. *Top. Curr. Chem.* **1994**, *170*, 83−111.
(17) Hilt, G.; Jarbawi, T.; Steckhan, E. *Chem. Eur. J.* **1997**, *3*, 79−88.
(18) Schröder, I.; Vasic-Racki, D.; Wandrey, C.; Liese, A. *Proc. Electrochem. Soc.* **2001**, *14*, 109−112.
(19) Liese, A.; Karutz, M.; Kamphuis, J.; Wandrey, C.; U. *Kragl Biotechnol. Bioeng.* **1996**, *51*, 544−550.
(20) Kruse, W.; Kragl, U.; Wandrey, C. German Patent Application DE4436149,-1998.
(21) Nishise, H.; Nagao, A.; Tani, Y.; Yamada, H. *Agric. Biol. Chem.* **1984**, *48*, 1603−1609.
(22) Scott, S. L.; Chen, W.-J.; Bakac, A.; Espenson, J. H. *J. Phys. Chem.* **1993**, *97*, 6710−6714.

10.1021/op034122y CCC: $27.50
Published on Web 01/28/2004

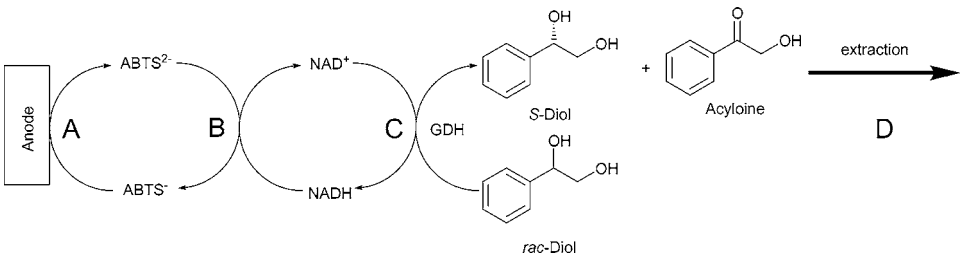

Figure 1. **Reaction system of the oxidative kinetic racemic resolution with in situ regeneration of the oxidized cofactor NAD^+ by anodic oxidation mediated by the ABTS redox couple (GDH: glycerol dehydrogenase).**

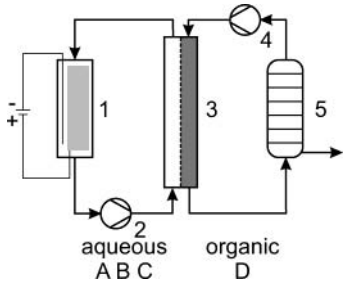

Figure 2. **Modified E^3MR with electrochemical cofactor oxidation electrochemical flow cell (1), aqueous circuit pump (2), ultrafiltration/extraction module (3), organic circuit pump (4), continuous distillation (5).**

fast and selective oxidant for regeneration of NAD^+.[18] The overall reaction is depicted in Figure 1. A simplified setup for the E^3MR combining extraction and ultrafiltration using a solvent-stable ultrafiltration module[8] was utilized (Figure 2).

Complete numerical description of the system is often impossible, partly because the nature of the overall reaction setup is complex and there is a relatively small amount of data obtained by initial rate measurements; furthermore the actual reaction conditions may differ from characterization conditions. Due to the complex nature of the reaction system, simulations of the system were hampered. Therefore a model was built on the basis of independent characterizations of the relevant processes and modules. This model was refined by experimental data to account for influences under reaction conditions, which cannot be covered by independent initial rate experiments. The model consists of a system of ordinary differential equations. To some extent it is able to describe the concentration courses, as well as the process quantities, i.e., conversion and enantiomeric excess. To this end, it was necessary to take experimentally obtained enzyme activity and the cofactor dosage into account. The model was further used to extrapolate possible changes to the experimental conditions.

2. Experimental Section

2.1. General. 2,2′-Azinobis(3-ethylbenzothiazoline-6-sulfonate) diammonium salt, glycerol and all buffer salts were supplied by Sigma-Aldrich, Steinheim, Germany. NADH was obtained from Biomol, Hamburg, Germany. NAD^+, glycerol dehydrogenase from *Cellulomonas* spp. (GDH, EC 1.1.1.6), and formate dehydrogenase from *Candida boidinii* (FDH, EC 1.2.1.2) were purchased from Jülich Fine Chemicals, Jülich, Germany. All chemicals employed were of the highest purity available and used without further purification. All solutions were prepared from deionized water, obtained by nanofiltration (Milli-Q, Millipore, Germany). Carbonate buffer was prepared by adjusting a solution of potassium bicarbonate (0.1 M) with a solution of dipotassium carbonate (0.1 M). This buffer solution was used at pH = 9.0 unless otherwise stated. 2-Hydroxyacetophenone was prepared according to a procedure described elsewhere.[25,26] UV spectrometry was carried out at 25 °C on a Spectrophotometer UV 160 (Shimadzu Europe, Duisburg, Germany) using quartz cuvettes (d = 1 cm) or on a microplate reader (Thermo max, Molecular Devices, Heidelberg, Germany) using 96-well plates. Protein content was determined as described in the literature.[27−29] Conversion and enantiomeric excess (enantiomeric ratio) were monitored using an HP6890 gas chromatograph (Agilent Technologies, Waldbronn, Germany), equipped with a CP-Chirasil-Dex CB column (Varian, Darmstadt, Germany), with racemic 1-phenyl-1,2-ethanediol used as a standard (carrier gas: hydrogen, gas flow: 140 mL/min, pressure: 0.5 bar, isotherm 130 °C, 35 min, typical retention times: 2-hydroxyacetophenone: 5.7 min, (*S*)-1-phenyl-1,2-diol: 23.2 min, (*R*)-1-phenyl-1,2-diol: 24.8 min).

2.2. Cyclic Voltammetry. Cyclic voltammetric experiments were performed on a BAS 100 B/W Version 2.3 Electrochemical Workstation (Bioanalytical Systems, West Lafayette, Indiana, U.S.A.) using a three-electrode electrochemical cell. The working electrode was a glassy carbon disk (3-mm diameter), and platinum wire was used as the counter electrode. All potentials were measured and quoted versus Ag|AgCl|3 M KCl as a reference electrode.

The experiments were carried out at 25 °C after degassing the solution with high-purity helium under nitrogen atmosphere. Prior to each experiment, the working electrode was polished mechanically to a mirror finish using 0.05 μm alumina powder and rinsed with deionized water followed by buffer. The reduced cofactor was added as a solid and the solution stirred between experiments.

2.3. Electrochemical Oxidation of $ABTS^{2-}$ to $ABTS^{\bullet-}$. Electrochemical oxidation was performed in a quasi-divided flow cell. The glass flow cell was equipped with a thermo-

(23) Kragl, U.; Liese, A. In *The Encyclopedia of Bioprocess Technology: Fermentation, Biocatalysis & Bioseparation*; Flickinger, M. C., Drew, S. W., Eds.; John Wiley & Sons: New York, 1999; pp 454−464.
(24) Kragl, U. Kruse, W.; Hummel, W.; Wandrey, C. *Biotechnol. Bioeng.* **1996**, *52*, 309−319.
(25) Madelung, W.; Oberwegner, M. E. *Chem. Ber.* **1932**, *65*, 931−941.
(26) Cebrián, G. R. *An. Soc. Espan. [B]* **1948**, *44*, 587−592.
(27) Re, R.; Pellegrini, N.; Proteggente, A.; Pannala, A.; Yang, M.; Rice-Evans, C. *Free Radical Biol. Med.* **1999**, *26*, 1231−1237.
(28) Pinkernell, U.; Nowack, B.; Gallard, H.; von Gunten, U. *Water Res.* **2000**, *34*, 4343−4350.
(29) Sedmark, J. J.; Grossberg, S. E. *Anal. Biochem.* **1977**, *79*, 544−552.

stating jacket. The anode was prepared from rolled graphite felt (Sigratherm, 4 mm, 26.5 cm × 8.5 cm, 4.6 g, SGL carbon, Bonn, Germany) contacted with platinum wire. The counter electrode (Pt-wire in a dialysis tube to prevent direct electrical contact) and the pseudoreference electrode (Ag-wire in a dialysis tube to prevent direct electrical contact) were placed in the center. Circulation was established using a peristaltic pump (Watson-Marlow GmbH, Germany). The cell was thermostated to 25 °C. Potentiostatic electrolysis was performed at 0.585 V (Amel potentiostat model 553, Milan, Italy) and absorbance of the radical cation 420 nm[27,28] was measured online in a flow cell (d = 1.5 mm) in a UV photospectrometer (AD2000, Avantes, Netherlands).

2.4. Reaction of $ABTS^{\bullet -}$ with NADH. The reaction was followed by detecting the decrease in absorbance of $ABTS^{\bullet -}$ (0.01 M in buffer), prepared by electrolysis of $ABTS^{2-}$ at 585 mV vs Ag/AgCl at 420 nm,[24,25] upon the addition of NADH at varying concentrations.

2.5. Stability Measurements. *2.5.1. NAD^+.* A solution of 1 mM NAD^+ in potassium carbonate buffer was thermostated at 25 °C. The NAD^+ concentration was measured after reduction by formate dehydrogenase (FDH, EC 1.2.1.2) according to the following procedure. The NAD^+ solution (0.1 mM) was allowed to react with FDH (0.06 mg/mL) in 0.1 potassium formate solution at pH = 7.0 and 25 °C for 10 min. Absolute concentrations of NADH were determined by UV spectrometry at 340 nm.

2.5.2. NADH. A solution of 0.5 mM NADH in buffer was stored at 25 °C. Samples were analyzed for NADH concentration by UV spectrometry.

2.5.3. GDH. A solution of 2 mg/mL GDH in buffer was stored at 25 °C. Samples of this solution were withdrawn and analyzed for enzyme activity towards glycerol. A solution of 20 mM glycerol and 2 mM NAD^+ in buffer was monitored for change in absorbance at 340 nm after addition of the enzyme.

2.6. Characterization of GDH. The reaction was followed by monitoring increase in absorbance of NADH at 340 nm at 25 °C in buffer. The reaction was initiated by addition of GDH (0.26 mg/mL). Standard concentrations were racemic 1-phenyl-1,2-ethanediol 100mM; NAD^+: 2 mM. Concentrations were varied to obtain kinetic data.

2.7. Extraction. A solution of 1 mg/mL 1-phenyl-1,2-ethanediol and 0.3 mg/mL 2-hydroxy-1-phenylpropanone (300 mL) was pumped (0.5 L/min) through the hollow fibers of the extraction module (Minikros-module, 8000 cm^2 surface area, PS, MWCO 10 kD, membrapure, Germany, peristaltic pump: Watson-Marlow GmbH, Germany), whereas isooctane was pumped through the outer shell of the extraction module in counter-current flow (13 mL/min, pump: telab, Germany) (Figure 2). The organic solvent (500 mL) was continuously distilled from the extracted compounds under reduced pressure (180 ± 10 mbar, 65 °C, Rotavapor RE 111, Vacobox R-160, Büchi GmbH, Göppingen, Germany).

2.8. E^3MR Experiment. The reaction was carried out by combining the electrolytic cell and extraction module in series as shown in Figure 2. A buffered solution of 1-phenyl-1,2-ethanediol (300 mL, 33 mM), 0.4 mM NAD^+, 0.56 units/mL GDH (18 units/mg) and 0.2 mM $ABTS^{2-}$ was used as the aqueous phase. Initial concentrations were $[R\text{-diol}]_0$ = 16.5, $[NAD^+]_0$ = 0.4, [NADH] = 0.0, $[ABTS^{2-}]_0$ = 0.2, and $[ABTS^{\bullet -}]_0$ = 0.0. The reaction was started by raising the electrolysis potential to the desired value. Cofactor was replenished at 0, 28.4, 53.2, 166.5, and 199.2 h with 0.4, 0.2, 1.3, 0.5, and 0.3 mM, respectively. Enzyme activity is indicated in Figure 3. Samples were periodically withdrawn and analyzed for protein content, residual enzyme activity, concentration, enantiomeric ratio (S/R), and enantiomeric excess ($(S - R)/(S + R)$) of diol and hydroxyketone.

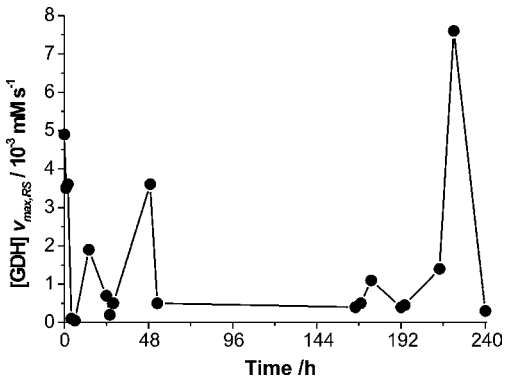

Figure 3. **Enzymatic activity during the course of the E^3MR experiment. The increases in the enzyme activity over time result from supplementing enzyme at 16, 53,166, and 199 h.**

2.9. Simulation. The model parameters were obtained by analysis of the independent experiments preceding the E^3MR experiment, as described above. The unadjusted parameters were employed for simulation of the E^3MR experiment, i.e., none of the parameters was adapted by fitting the simulated curves to the experimental ones. The simulations were carried out using Maple 7 (Waterloo Maple Inc.). The numerical solution was found using the embedded Livermore Stiff ODE solver, lsode.

3. Results and Discussion

3.1. Five steps contributing significantly to reaction rate and selectivity were identified (Figure 1):

(A) heterogeneous formation of the radical cation $ABTS^{\bullet -}$ from $ABTS^{2-}$,

(B) homogeneous oxidation of NADH to NAD^+ by the radical cation,

(C) enzyme-catalyzed oxidation of 2-phenylpropane-1,2-diol (*rac*-diol),

(D) extraction of the inhibiting hydroxyketone from the reaction mixture,

(E) decay of the enzyme and the cofactor under reaction conditions.

These steps corresponding to the modules used in the overall setup were then characterized independently.

A batch experiment in the electrochemical E^3MR was carried out. This experiment was then simulated with the kinetic parameters of the five steps as characterized by the inital rate experiments,[18] taking into account measurements of enzyme activity and the adjustments of enzyme and cofactor concentration during the experiment. Different

Table 1. **Rate laws for the individual steps of the overall oxidative racemic resolution**

	rate law	reaction step
A	$k_{ABTS}{}^{2-}[ABTS^{2-}]$	$ABTS^{\bullet-}$ formation
B	$k_{NADH}\,[NADH][ABTS^{\bullet-}]$	homogeneous oxidation
C-*R*	$\dfrac{[GDH]\upsilon_{max,R}\,[R\text{-diol}][NAD^+]}{\left(K_{m,R}\left(1+\dfrac{[acyloin]}{K_{i,acyloin}}\right)+[R\text{-diol}]\right)\left(K_{m,NAD}\left(1+\dfrac{[NADH]}{K_{i,NADH}}\right)+[NAD^+]\right)}$	oxidation of *R*-diol
C-*S*	$\dfrac{[GDH]\upsilon_{max,S}\,[S\text{-diol}][NAD^+]}{\left(K_{m,S}\left(1+\dfrac{[acyloin]}{K_{i,acyloin}}\right)+[S\text{-diol}]\right)\left(K_{m,NAD}\left(1+\dfrac{[NADH]}{K_{i,NADH}}\right)+[NAD^+]\right)}$	oxidation of *S*-diol
D-*R*	$k_{ex,diol}\,[R\text{-diol}]$	diol extraction
D-*S*	$k_{ex,diol}\,[S\text{-diol}]$	
D-acyloin	$k_{ex,acyloin}\,[acyloin]$	acyloin extraction
E-NAD^+	$k_{d,NAD}\,[NAD^+]$	NAD^+ decay
E-NADH	$k_{d,NADH}\,[NADH]$	NADH decay

Table 2. **Kinetic constants used for the simulation and for testing the steady-state assumption**

parameter	value	unit
[GDH] $\upsilon_{max,S}$	1.4×10^{-3}	mM s^{-1}
[GDH] $\upsilon_{max,R}$	1.0×10^{-2}	mM s^{-1}
$K_{m,R}$	15.6 ± 0.7	mM
$K_{m,S}$	51.0 ± 0.8	mM
$K_{m,NAD}$	0.71 ± 0.04	mM
$K_{i,acyloin}$	$(0.20 \pm 0.05) \times 10^{-6}$	mM
$k_{ex,diol}$	$(0.24 \pm 0.06) \times$	s^{-1}
$k_{ex,acyloin}$	$(0.67 \pm 0.03) \times 10^{-5}$	s^{-1}
$k_{d,NAD}$	$(0.59 \pm 0.05) \times 10^{-5}$	s^{-1}
[GDH] $\upsilon_{max,RS}{}^a$	5.82×10^{-3}	mM s^{-1}
$K_{m,RS}{}^a$	25.0 ± 0.5	mM
$k_{d,NADH}{}^a$	$(0.66 \pm 0.04) \times 10^{-6}$	s^{-1}
$k_{NADH}{}^a$	$(6.4 \pm 0.1) \times 10^3$	$M^{-1}\,s^{-1}$
$k_{ABTS}{}^{2-\,a}$	$(1.28 \pm 0.07) \times 10^{-2}$	s^{-1}

[a] Only used for testing the steady-state assumption.

parameters were then altered to extrapolate the results to other conditions to gain insight into the system and identify possible limitations to be overcome.

3.1.1. Formation of ABTS$^{\bullet-}$. The oxidation of $ABTS^{2-}$ to the teal-colored $ABTS^{\bullet-}$ takes place in the electrochemical flow cell (Figure 2). We characterized the influence of flow rate as operating under conditions not limited by mass transfer. Under experimental conditions (0.6 L/min, $[ABTS^{2-}]_0 = 0.19$ mM) the oxidation rate is a linear function of $ABTS^{2-}$ concentration and thus can be described by a pseudo-first-order rate law with the first-order rate constant $k_{f,ABTS^{\bullet-}}$. The reaction rate laws and the respective rate constant are shown in Tables 1 and 2.

3.1.2. Homogeneous Oxidation. In the investigated concentration range, homogeneous oxidation of NADH to NAD^+ by the radical cation was determined as first order in both reactants with the rate constant k_{NADH}. Due to the stoichiometry, two molecules of $ABTS^{\bullet-}$ are needed for the two-electron step. The reaction order with respect to $ABTS^{\bullet-}$ could not be determined accurately and is under investigation. We assume the first oxidation step to be rate limiting and that successive oxidation is fast.

3.1.3. Enzyme Catalysis. The enzyme-catalyzed regio- and enantioselective oxidation of the racemic 1-phenyl-1,2-ethanediol (*rac*-diol)) to acyloin was determined by initial rate experiments. It can be described by Michaelis−Menten-type kinetics for both enantiomers with limiting reaction rates $\upsilon_{max,S}$ and $\upsilon_{max,R}$, respectively, and complex binding constants $K_{m,S}$ and $K_{m,R}$. As the oxidation product, acyloin inhibits both reactions and is accounted for by the inhibition constant $K_{i,acyloin}$. Values from the nonlinear regression of the initial rate measurements with the rate equations are given in Tables 1 and 2.

3.1.4. Extraction. Extraction of diol and acyloin from the aqueous phase can be described by a first-order rate law with rate constants $k_{ex,diol}$ and $k_{ex,acyloin}$, respectively (Table 2). The extraction is strongly dependent on the organic solvent, and in the case of iso-octane a selectivity of 28 for the extraction of the more lipophilic product acyloin can be achieved. The usage of *n*-octane, for example, is rather unselective. The choice of solvent is mainly hampered by the phase contactor, which is unstable with respect to other solvents of choice. Since this is due to the instability of sealings and the housing, further improvements can be predicted. Only commercial phase contactors were used to maintain the generality of the approach.

3.1.5. Decay of Cofactor and Enzyme. The decay of NAD^+ and NADH can be described by first-order rate laws with the rate constants $k_{d,NAD}{}^+$ and $k_{d,NADH}$ (Table 2).

The storage stability of the glycerol dehydrogenase from *Cellumonas* spp. (GDH) was found to be high with a half-life time of more than 80 days (buffer, pH = 9.0, 25 °C). Under reaction conditions this stability decreased due to the deactivation in the hollow-fiber module.

Since loss in enzymatic activity during the E^3MR experiment was much higher than observed by stability tests preceding the experiment, the simulations based on such decay curves could not describe the experimental observations. Instead, enzymatic activity determined from samples from the reactor run was used (see Figure 3) rather than the first-order decay curves implied by the stability measurements. Increases in enzyme activity indicate the addition of

enzyme at 16, 53,166, and 199 h. Because the enzyme concentration was not accessible, it was decided to use the product of enzyme concentration [GDH] and υ_{max} for the simulations.

3.2. E³MR Experiment. The combination of an ultrafiltration and extraction step using a solvent-stable ultrafiltration module as phase contactor decreased the aqueous reactor volume by more than 50% compared to previous approaches.[8]

3.3 Simulation. *3.3.1. Examination of the Reactions Preceding the Enzymatic Catalysis.* Given the numerical values of the rate constants for the anodic and the homogeneous oxidation reaction it was investigated whether the steady-state assumption was valid for the treatment of these reactions.

For this purpose a system of ordinary differential equations (see eqs 1−7 and Tables 1 and 2) was formulated, whereas a first-order rate law was postulated for both compounds of the oxidation reaction as a first approximation. The $ABTS^{2-}$ concentration was less than 0.12 mM throughout the experiment.

$$\frac{d}{dt}[ABTS^{\bullet -}] = +A - B \quad (1)$$

$$\frac{d}{dt}[ABTS^{2-}] = -A + B \quad (2)$$

$$\frac{d}{dt}[NAD^+] = +B - C\text{-}R - C\text{-}S - E\text{-}NAD^+ \quad (3)$$

$$\frac{d}{dt}[NADH] = -B + C\text{-}R + C\text{-}S - E\text{-}NADH \quad (4)$$

$$\frac{d}{dt}[R\text{-diol}] = -C\text{-}R - D\text{-}R \quad (5)$$

$$\frac{d}{dt}[S\text{-diol}] = -C\text{-}S - D\text{-}S \quad (6)$$

$$\frac{d}{dt}[acyloin] = +C\text{-}R + C\text{-}S - D\text{-acyloin} \quad (7)$$

Using these parameters (Table 2) and initial concentrations (see above) the system of ordinary differential equations was integrated for the first 2.8 h. On the basis of this simulation, it was demonstrated that the NADH concentration was constant at a very low level (<0.01 mM) during the entire experiment and that after approximately 2.5 h the $ABTS^{\bullet -}$ concentration reached more than 0.99 of the initial $ABTS^{2-}$ concentration ($t_{1/2} \approx 0.1$ h). Not until k_{NADH} was decreased by a factor of 100 could interim formation of NADH (>0.01 mM) be simulated. Hence, the regeneration of NAD^+ (B) is fast under the experimental conditions and does not determine overall rate.

3.3.2. Simulation of the E³MR Experiment. Due to the previous modeling results, the equation for NADH, eq 4, and the ABTS redox couple, eqs 1 and 2, were omitted from the system of ordinary differential equations (ODE) (eqs 1−7). Furthermore, eq 3 could be reduced to the decay term $E\text{-}NAD^+$ since other contributions were shown to be negligible. Also the inibition by NADH for the oxidation can be neglected, because the inhibition term [NADH]/$K_{i,NADH}$ in the denominator of C-*R* and C-*S* is small. This highlights the advantage of electrochemical oxidative regeneration for the reaction, since the relatively strong inhibition by NADH ($K_{i,NADH}$ = 0.1 mM) can be neglected. The parameters and initial conditions used for the simulation thus were reduced to nine (Table 2), and the initial concentrations were as given above. The dosage profile of NAD^+ was taken as given above. Actual values of the enzymatic activity originated from the measured data (Figure 3). Since the activity was determined from the racemic substrate, the [GDH] υ_{max} values of the enantiomers were calculated by balancing the respective reaction rates with regard to assay conditions.

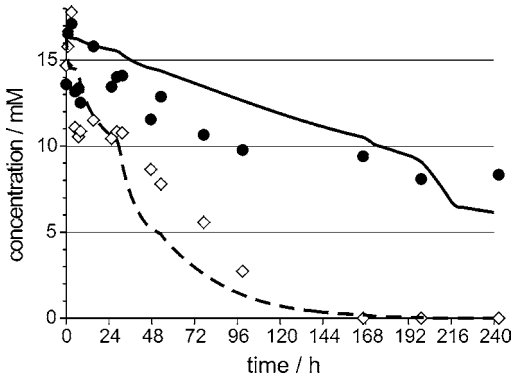

Figure 4. **Simulated (lines) and experimental concentrations (points) as a function of reaction time for *R*-diol (solid) and *S*-diol (dashed, open).**

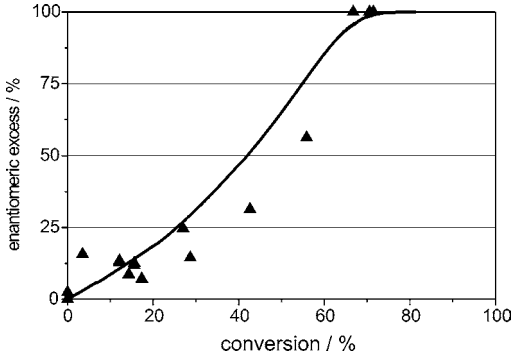

Figure 5. **Simulated (line) and experimental (points) enantiomeric excess as a function of conversion.**

The time courses of the related reactants resulted after integration of the ODE system within 0−242 h, see Figure 4.

The results for conversion and enantiomeric excess (ee) calculated from the simulated time courses are shown in Figure 5.

Whilst the simulated concentrations for *R*-diol adequately match the experimental points, the simulated *S*-diol concentrations deviate from the experimental data. This may be explained by the fact that $K_{i,acyloin}$ and $K_{m,NAD}$ values were not determined separately for each enantiomer. For the same reason, calculation of the [GDH] $\upsilon_{max,R}$ and [GDH] $\upsilon_{max,S}$ values from the [GDH] $\upsilon_{max,RS}$ value was imprecise.

Nevertheless, the model appears to be suitable for identifying the limiting parameters restricting conversion rate and enantiomeric excess. From sensitivity analysis it was demonstrated that the main influencing parameters are the inhibition constant $K_{i,acyloin}$ and the extraction coefficient $k_{ex,acyloin}$.

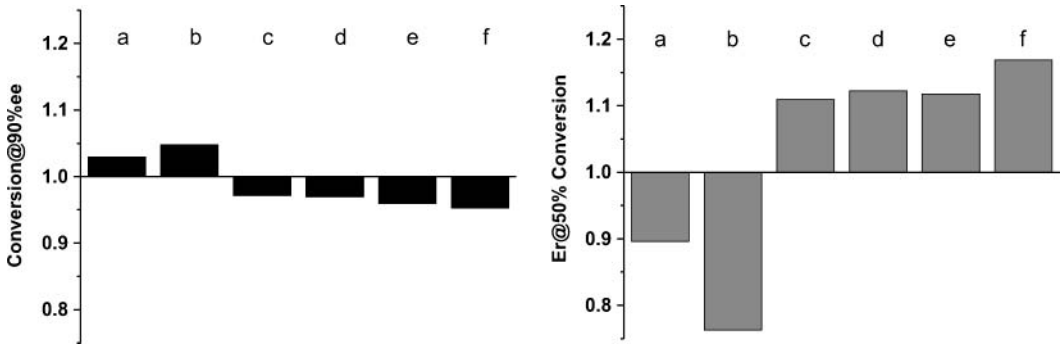

Figure 6. **Relative to the original model calculated conversion at 90% enantiomeric excess (left) and enantiomeric ratio at 50% conversion (right) are plotted as function of varying experimental conditions; (a) 2-fold initial concentration (2[PED]$_0$), (b) 4-fold initial concentration (4[PED]$_0$), (c) initial concentration [NAD$^+$]$_0$ = 3 mM with no further cofactor addition, (d) constant [NAD$^+$]$_t$ = 3 mM, (e) improved extraction for 2-hydroxyacetophenone (10 $k_{ex,ac}$), (f) no enzyme deactivation.**

3.4. Variation of Parameters. The model described above was used to make predictions for the experimental results obtained under modified process conditions.

Different approaches were formulated for the investigation of alternating process conditions, which could influence the experimental results. Kinetic constants of the enzyme were not altered, as these are outside our influence. Only one parameter was modified at a time so that the extrapolation would show the significance of that parameter alone and guide future efforts at improving the system. It is important to consider that the selectivity depends on the relative concentrations of the diols as well as the absolute concentrations of the diol. The results are shown in Figure 6.

- Initial substrate concentration (Figure 6a,b)

Doubling the initial concentration of 1-phenyl-1,2-ethanediol does not significantly affect conversion and ee. However, due to deactivation, the enzymatic activity was not high enough during the experiment for the transformation of the 4-fold diol concentration.

- NAD$^+$ dosage (Figure 6c,d)

Two alternative strategies were compared to the actual experiment. A 6-fold higher initial concentration with no supplemental dosage and a chemostatic approach with constant NAD$^+$ concentration were investigated. Both approaches could apparently improve the experimental results.

The use of an initial concentration of [NAD$^+$]$_0$ = 3.0 mM could significantly increase the ee. The high initial concentration of NAD$^+$ increases enzymatic reaction rate at the beginning of the experiment so that the high molar concentrations of *R*-diol available at that point in time could be rapidly transformed with better enantioselectivity. Towards the end of the experiment the small substrate amount predominantly limits the rate of the enzymatic conversion. Hence, keeping the NAD$^+$ concentration at a constant level of 3.0 mM could improve the experimental results.

- Extraction (Figure 6e)

Improving the extraction could strongly increase conversion and ee. A higher degree of extraction was simulated by an increase of the extraction constant $k_{ex,acyloin}$ by factor 10. This also changes selectivity towards the desired extraction of the lipophilic product. Alternate solvents may yield superior results, but the choice of solvents is reduced by the stability of commercially available membrane modules.

- Enzyme stability (Figure 6f)

The deactivation of the enzyme turned out to have the strongest influence. If deactivation was omitted from the simulation, results were significantly enhanced. Here also the use of a different solvent could be a suitable solution, even though stability measurements did not indicate such a drastic decrease of stability in the presence of the organic solvent. The increase in enantioselectivity is mainly thought to be attributable to increasing the reaction relative to the extraction rate. If the reaction can be carried out on a shorter time scale, the concentrations of the diol are higher in the simulated experiment since extraction rate is unchanged. As the enantioselectivity decreases with the concentration of the substrate, a faster reaction favors selectivity.

4. Conclusions

The ABTS-redox couple is a fast mediator for the electrochemical cofactor regeneration of NAD$^+$. Utilization of the E^{3}MR is a feasible solution to overcome product inhibition for the oxidation of 1,2-hydroxyketones to obtain the desired enantiopure *S*-diol from oxidative racemic resolution. The model enzyme system is far from being optimal or of practical relevance. This holds true for both stability under reaction conditions and stereoselectivity, which can be emphasized by means of simulation. It is also demonstrated that the electrochemical regeneration does not limit the overall rate, whereas the extraction and the replenishment strategy should be the targets of new investigations. The simulation proved to be a powerful tool for determining the significant parameters in such a multistep setup.

Acknowledgment

We thank U. Kragl (Universität Rostock) for valuable discussions. For financial support, thanks are due to BASF AG, Ludwigshafen, Germany.

Supporting Information Available

Experimental details. This material is available free of charge via the Internet at http://pubs.acs.org.

Received for review August 27, 2003.

OP034122Y